Polarization coupling in a highly birefringent photonic crystal fiber by torsional acoustic wave

Kwang Jo Lee,* Kee Suk Hong, Hyun Chul Park, and Byoung Yoon Kim

Department of Physics, Korea Advanced Institute of Science and Technology
373-1 Guseong-dong, Yuseong-gu, Daejeon, 305-701, Korea
** kjl@kaist.ac.kr*

Abstract: We demonstrate and analyze the acousto-optic coupling between two optical polarization modes of the LP_{01} mode propagating in a highly birefringent photonic crystal fiber. The coupling is realized based on wavelength selective acousto-optic coupling by traveling torsional acoustic wave in an all-fiber tunable polarization filter configuration. The dispersion properties of the torsional acoustic wave in the photonic crystal fiber and the influence of axial non-uniformity in the modal birefringence on the filter transmission are discussed in detail.

OCIS codes: (060.2310) Fiber optics; (060.5295) Photonic crystal fibers; (230.1040) Acousto-optical devices.

References and links

1. P. St. J. Russell, "Photonic crystal fibers," Science **299**, 358-362 (2003).
2. J. C. Knight, "Photonic crystal fibres," Nature **424**, 847-851 (2003).
3. P. St. J. Russell, "Photonic-crystal fibers," J. Lightwave Technol. **24**, 4729-4749 (2006).
4. H. Ebendorff-Heidepriem, K. Furusawa, D. R. Richardson, and T. M. Monro, "Fundamentals and applications of silica and nonsilica holey fibers," Proc. SPIE **5350**, 35-49 (2004).
5. J. Lægsgaard and A. Bjarklev, "Microstructured optical fibers – fundamentals and applications," J. Am. Ceram. Soc. **89**, 2-12 (2006).
6. A. Diez, T. A. Birks, W. H. Reeves, B. J. Mangan, and P. St. J. Russell, "Excitation of cladding modes in photonic crystal fibers by flexural acoustic waves," Opt. Lett. **25**, 1499-1501 (2000).
7. M. W. Haakestad and H. E. Engan, "Acoustooptic properties of a weakly multimode solid core photonic crystal fiber," J. Lightwave Technol. **24**, 838-845 (2006).
8. M. W. Haakestad and H. E. Engan, "Acoustooptic characterization of a birefringent two-mode photonic crystal fiber," Opt. Express **14**, 7319-7328 (2006), http://www.opticsinfobase.org/abstract.cfm?URI=oe-14-16-7319.
9. D. -I. Yeom, P. Steinvurzel, B. J. Eggleton, S. D. Lim, and B. Y. Kim, "Tunable acoustic gratings in solid-core photonic bandgap fiber," Opt. Express **15**, 3513-3518 (2007), http://www.opticsinfobase.org/abstract.cfm?URI=oe-15-6-3513.
10. H. S. Kim, S. H. Yun, I. K. Hwang, and B. Y. Kim, "All-fiber acousto-optic tunable notch filter with electronically controllable spectral profile," Opt. Lett. **22**, 1476-1478 (1997).
11. K. J. Lee, D. -I. Yeom, and B. Y. Kim, "Narrowband, polarization insensitive all-fiber acousto-optic tunable bandpass filter," Opt. Express **15**, 2987-2992 (2007), http://www.opticsinfobase.org/abstract.cfm?URI=oe-15-6-2987.
12. K. J. Lee, H. C. Park, and B. Y. Kim, "Highly efficient all-fiber tunable polarization filter using torsional acoustic wave," Opt. Express **15**, 12362-12367 (2007), http://www.opticsinfobase.org/abstract.cfm?URI=oe-15-19-12362.
13. H. E. Engan, B. Y. Kim, J. N. Blake, and H. J. Shaw, "Propagation and optical interaction of guided acoustic waves in two-mode optical fibers," J. Lightwave Technol. **6**, 428-436 (1988).
14. K. F. Graff, *Wave Motion in Elastic Solids* (Ohio State University Press, 1975), Chap. 2.
15. S. P. Timoshenko and J. N. Goodier, *Theory of Elasticity* (McGrow-Hill, 1970), Chap. 10.
16. S. Johnson and J. Joannopoulos, "Block-iterative frequency-domain methods for Maxwell's equations in a planewave basis," Opt. Express **8**, 173-190 (2001), http://www.opticsinfobase.org/abstract.cfm?URI=oe-8-3-173.
17. S. G. Johnson and J. D. Joannopoulos, "The MIT photonic-bands (MPB) package," http://ab-initio.mit.edu/wiki/index.php/MIT_Photonic_Bands.
18. B. Langli and K. Bløtekjær, "Effect of acoustic birefringence on acoustooptic interaction in birefringent two-mode optical fibers," J. Lightwave Technol. **21**, 528-535 (2003).

#91710 - $15.00 USD Received 14 Jan 2008; revised 15 Mar 2008; accepted 15 Mar 2008; published 19 Mar 2008

19. H. E. Engan, "Analysis of polarization-mode coupling by acoustic torsional waves in optical fibers," J. Opt. Soc. Am. A **13**, 112-118 (1996).
20. D. Östling and H. E. Engan, "Narrow-band acousto-optic tunable filtering in a two-mode fiber," Opt. Lett. **20**, 1247-1249 (1995).
21. D. A. Smith, A. d'Alessandro, J. E. Baran, and H. Herrmann, "Source of sidelobe asymmetry in integrated acousto-optic filters," Appl. Phys. Lett. **62**, 814-816 (1993).
22. F. Chollet, J. P. Goedgebuer, and G. Ramantoko, "Limitations imposed by birefringence uniformity on narrow-linewidth filters based on mode coupling," Opt. Eng. **40**, 2763-2770 (2001).
23. H. Herrmann and St. Schmid, "Integrated acousto-optical mode-convertors with weighted coupling using surface acoustic wave directional couplers," Electron. Lett. **28**, 979-980 (1992).
24. W. Warzanskyj, F. Heismann, and R. C. Alferness, "Polarization-independent electro-optically tunable narrow-band wavelength filter," Appl. Phys. Lett. **53**, 13-15 (1988).
25. F. Laurell and G. Arvidsson, "Frequency doubling in Ti:MgO:$LiNbO_3$ channel waveguides," J. Opt. Soc. Am. B **5**, 292-299 (1988).

1. Introduction

Photonic devices using the photonic crystal fibers (PCFs) have attracted increasing attention because of their unique optical properties and design flexibility that cannot be achieved in conventional optical fibers, such as a wide range of single-mode operation, dispersion tailoring, reduced or enhanced effective nonlinearity, bandgap guidance, and easily attainable high birefringence [1, 2]. This opens up diverse potential applications including high power delivery, optical amplification, optical sensing, and low non-linear data transmission in optical communication, metrology, medicine, and beyond [3-5]. One of such device category of interest is all-fiber acousto-optic (AO) devices using PCFs because their design flexibility in fiber parameters can make it possible to realize tunable filters with wide- or narrow-bandwidth, and an extremely wide wavelength tuning range [6-9]. In addition to the advantages of conventional all-fiber acousto-optic tunable filters (AOTFs), such as low insertion loss, wide and fast wavelength tuning, and variable attenuation with simple electronic control [10, 11], the flexibility obtained by PCFs will expand the application of such devices. AO coupling properties in several types of PCFs have been investigated in a single mode PCF [6], a weakly multimode solid core PCF [7], a birefringent two-mode PCF [8], and a fluid-filled solid-core photonic bandgap fiber (PBGF) [9]. However, all of the reported results to date on the AO coupling in PCFs are based on AO coupling between several spatial modes using traveling flexural acoustic wave.

Recently, we reported a practical all-fiber acousto-optic tunable polarization filter (AOTPF) based on the polarization mode coupling in LP_{01} mode in a conventional highly birefringent (HB) optical fiber using traveling torsional acoustic wave [12]. In this paper, we demonstrate and analyze, for the first time to our knowledge, the AO coupling between two optical polarization modes of the LP_{01} mode propagating in a HB PCF. A full coupling between two polarization modes was achieved over the wavelength range from 1530 nm to 1620 nm in an all-fiber AOTPF using the lowest order torsional acoustic mode. The transmission properties of the fabricated filter and the dispersion properties of the lowest order torsional acoustic mode in the PCF are discussed in detail.

2. Acoustic and optical properties of the HB PCF

A cylindrical optical fiber, whose diameter is much smaller than acoustic wavelengths, can support longitudinal, flexural and torsional acoustic fundamental modes propagating along the fiber without cut-off [13]. Recent report shows that the presence of the air-hole structure in a PCF slightly changes the acoustic properties of the fiber as compared to the case of a standard solid fiber. For instance, the flexural acoustic wavelength in a PCF becomes smaller by ~ 1 % than that in a conventional fiber with the same outer diameter [7]. We discuss here the dispersion properties of the lowest-order torsional acoustic mode which can efficiently produce AO coupling between two polarization modes in a HB PCF. Figure 1 shows the schematic of the HB PCF subjected to oscillating end torques. The equation of motion for the

#91710 - $15.00 USD Received 14 Jan 2008; revised 15 Mar 2008; accepted 15 Mar 2008; published 19 Mar 2008

lowest order torsional acoustic mode and its propagation velocity in the fiber can be expressed as,

$$C\frac{\partial^2\theta}{\partial x^2} = \rho J\frac{\partial^2\theta}{\partial t^2}, \tag{1}$$

$$V_s = \sqrt{\frac{C}{\rho J}}, \tag{2}$$

respectively [14]. Here, C, J, and ρ denote the torsional rigidity, the polar moment of inertia, and the density of the fiber, respectively.

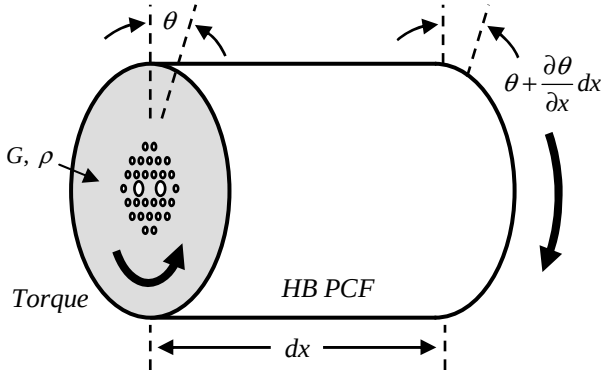

Fig. 1. Differential element of the HB PCF subjected to end torque. θ denotes the angle of twist.

The torsional rigidity means the resistance of the fiber to twist and, for a rod of circular cross-section, it is given by the product of the polar moment of inertia (J) and the shear modulus (G). The polar moment of inertia and the shear modulus mean the geometrical factor of the ability to resist torsion and the corresponding material factor, respectively. In case of the radially non-homogeneous circular cylinder in the cross-section, such as the PCF, the shear modulus and the fiber density are given by

$$G(\vec{r}) = \begin{cases} G, & \text{pure silica region} \\ 0, & \text{air-hole region} \end{cases} \text{ and } \rho(\vec{r}) = \begin{cases} \rho, & \text{pure silica region} \\ 0, & \text{air-hole region} \end{cases}, \tag{3}$$

respectively. Therefore, the torsional rigidity and the denominator of the Eq. (2) are expressed as the following integral form,

$$C \equiv \int_S G(\vec{r})r^2 dA = G\int_{S'} r^2 dA, \tag{4}$$

$$\rho J \to \int_S \rho(\vec{r})r^2 dA = \rho\int_{S'} r^2 dA, \tag{5}$$

in the all cross-sectional area S and the area of pure silica region S', respectively [15]. Here, dA and r denote an elemental area and the radial distance to the element dA from the fiber center, respectively. If we substitute Eq. (4) and Eq. (5) into Eq. (2), the geometrical factors are exactly canceled in the Eq. (2) and the propagation velocity of the lowest order torsional acoustic mode in the PCF is reduced to $V_s = (G/\rho)^{1/2}$, which is equal to the constant shear-wave velocity. As a result, the presence of the air-hole structure in the fiber cross-section does not change the dispersion properties of the lowest order torsional acoustic mode in the PCF, and the propagation velocity depends only on the material factors such as the fiber density and

#91710 - $15.00 USD Received 14 Jan 2008; revised 15 Mar 2008; accepted 15 Mar 2008; published 19 Mar 2008

the shear modulus. Therefore, as is the case of the standard optical fiber, the lowest order torsional acoustic mode can propagate along the PCF for all acoustic frequencies and wave numbers with a constant velocity equal to the shear-wave velocity, which is simply given by the product of the acoustic frequency and the corresponding wavelength of the torsional acoustic wave.

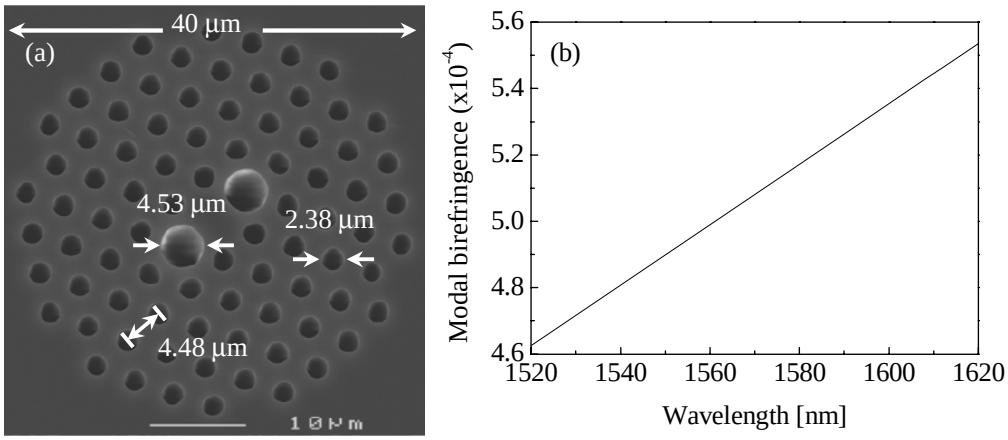

Fig. 2. (a) Scanning electron microscope (SEM) image of the cross-section a HB PCF, showing the period of hole-lattice and the diameters of the large hole and the small hole, and (b) Modal birefringence between two polarization eigenmodes of the LP_{01} mode in the HB PCF as a function of the optical wavelength.

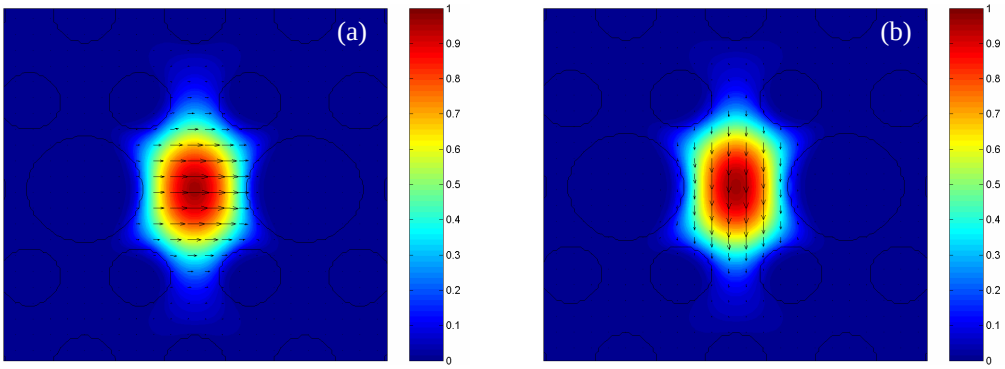

Fig. 3. Transverse electric (TE) field distributions of the two polarization eigenmodes of LP_{01} mode. The color level and the arrow denote the amplitude and the direction of the electric field, respectively.

Figure 2(a) shows the scanning electron microscope (SEM) image of the cross-section of the HB PCF used in the experiment. The HB PCF (L_B = 3.15 mm @ 1550 nm) is the index guiding type with a solid silica core surrounded by an array of air-hole with hexagonal symmetry and outer silica region. Optical birefringence is induced by two large air holes on the opposite sides of the core, which introduce a two-fold rotational symmetry into the fiber structure to obtain the form birefringence. The geometric parameters of the HB PCF are, as shown in Fig. 2(a), the hole-lattice period of 4.48 μm, the large hole diameter of 4.53 μm, and the small hole diameter of 2.38 μm, respectively. These parameters are estimated from the SEM images of the HB PCF cross section. The birefringence and modal properties of HB PCF were simulated with the MIT photonic-bands (MPB) package [16, 17], and the modal birefringence between two polarization eigenmodes of the LP_{01} mode in the HB PCF was shown in Fig. 2(b) as a function of the optical wavelength. Figure 3 shows the transverse

#91710 - $15.00 USD Received 14 Jan 2008; revised 15 Mar 2008; accepted 15 Mar 2008; published 19 Mar 2008

electric (TE) field distributions of the two polarization eigenmodes of LP_{01} mode. The color level and the arrow denote the amplitude and the direction of the electric field, respectively.

3. Polarization mode coupling in the HB PCF and the transmission properties of the fabricated filter

In case of the all-fiber AOTFs using traveling flexural acoustic wave, there are two possible origins of deterioration in the filter spectrum. The first is acoustic origin due to the variation of acoustic wavelength caused by non-uniformity of outer fiber diameter, and the other is optical origin due to the variation of optical beatlength caused by non-uniformity of refractive index profile in the optical fiber. In contrast to an all-fiber AOTF using flexural acoustic wave, torsional acoustic wave devices do not exhibit the coupling resonance shift or the deterioration in the filter spectrum caused by the axial non-uniformity of the outer fiber diameter or the undesirable ellipticity of the fiber cross-section [8, 18]. This comes from the fact that the acoustic wavelength of the lowest order torsional acoustic mode which provides phase matching condition for efficient polarization coupling is independent of the fiber diameter [19]. Therefore, the all-fiber AOTPFs using traveling torsional acoustic wave have no acoustic origin of deterioration in the filter spectrum. In addition, the AOTPF can easily be operated as a notch type or a bandpass type filter by adjusting the direction of the output polarizer, without any additional modification in the experimental setup [12].

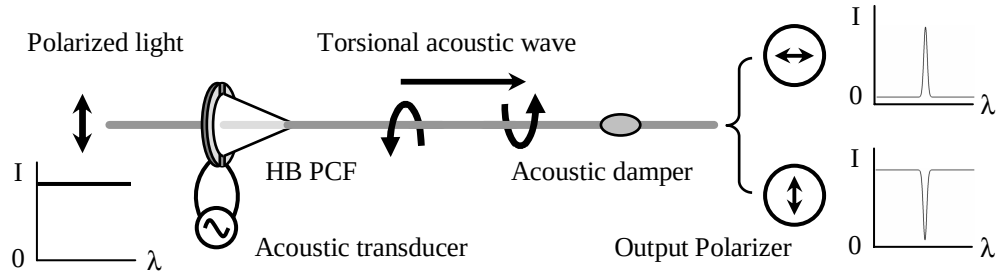

Fig. 4. Schematic of an all-fiber acousto-optic tunable polarization filter.

The schematic of an AOTPF was shown in Fig. 4 and its basic configuration is similar to that described in [12]. The device is composed of a torsional acoustic transducer, two polarizers, and the HB PCF. The input polarization state of the LP_{01} mode was aligned to one of the polarization eigenstate using the in-line fiber polarizer. The torsional acoustic wave was generated by the combination of two shear mode lead zirconate titanate (PZT) plates attached to one end of an acoustic horn with epoxy adhesive. The cylindrical acoustic horn is made of silica glass, whose outer diameter and length are 5 mm and 10 mm, respectively. The two PZT plates were arranged so that they oscillate 180 degrees out of phase. The generated torsional acoustic wave was coupled to a bare section of the HB PCF bonded to the central hole in the acoustic horn, and was absorbed by an acoustic damper (a sticky tape) at the end of the interaction region. The torsional acoustic wave has only the circumferential angular displacement component in the cross-section of the fiber. The periodic twists of the optical polarization eigenaxes in the HB PCF induced by the torsional acoustic wave perturb the incident polarization eigenstate of the LP_{01} mode and cause the energy to be transferred efficiently between two polarization eigenmodes. The AO coupling between two polarization modes is mainly caused by this geometrical twist effect, and that is reduced by 8% due to the elasto-optic effect [12, 19]. The incident eigen polarization of the LP_{01} core mode is converted to the other eigen polarization of the same core mode at resonant wavelength satisfying the phase matching condition that the acoustic wavelength is the same as beatlength between two polarization eigenmodes, as the following:

$$\left|\beta_{01,x} - \beta_{01,y}\right| = 2\pi / L_B \ , \tag{6}$$

#91710 - $15.00 USD Received 14 Jan 2008; revised 15 Mar 2008; accepted 15 Mar 2008; published 19 Mar 2008

where, L_B is the beatlength and β's denotes the wave number for two eigen polarizations of the LP_{01} mode. The beatlength is a function of wavelength and, for a given acoustic frequency, a specific wavelength component will be filtered in the device. The resonant wavelength and the transmitted power of the filter can be tuned by adjusting the frequency and the magnitude of the applied electric signal, respectively. Because the converted polarization mode can be selected or removed by adjusting the polarization direction of the output polarizer, the fabricated filter can be operated as the notch type or the bandpass type as illustrated in Fig. 4.

Figure 5 shows the measured transmission spectra of the AOTPF operating as the notch type [Fig. 5(a)] and as the bandpass type [Fig. 5(b)] at the applied acoustic frequency of 1.24 MHz. The achieved maximum coupling efficiency was 100% and the measured 3-dB optical bandwidth for a 60-cm-long AO interaction region was 6.6 nm at the wavelength around 1550 nm, which is larger than the theoretical value of 3.9 nm calculated with the equation in [20]. The increased optical bandwidth and the strong asymmetry in the sidelobe spectra are due to the undesirable non-uniformity in the modal birefringence caused by the weak axial irregularity in the air-hole lattice of the HB PCF. The same phenomena are observed in the various optical devices based on the coupling between two orthogonal polarizations in a birefringent medium, such as the integrated AO filters [21-23], the electro-optic filters [24], and the nonlinear optical second harmonic generators [25].

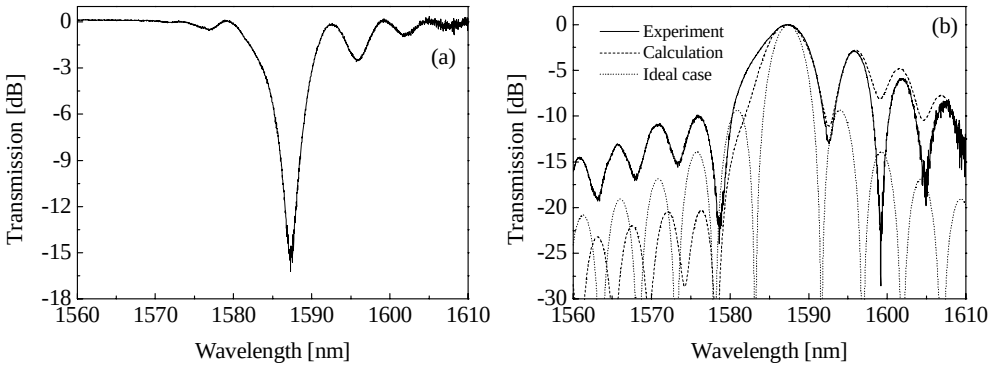

Fig. 5. Measured transmission spectra of the all-fiber AOTPF operating as (a) the notch type and as (b) the bandpass type at the acoustic frequency of 1.24 MHz. The measured and calculated transmission spectra for the quadratic Δn profile are shown with the ideal transmission curve in Fig. 5(b).

The degree of the axial non-uniformity in the modal birefringence which can account for the observed asymmetry in the sidelobe spectra can be estimated by the following approach. The resonant phase matching condition between two polarization modes is satisfied when the acoustic wavelength matches the optical polarization beatlength $L_B = \lambda/\Delta n$, where Δn is the modal birefringence between two polarization eigenmodes. If Δn is slightly not uniform along the longitudinal axis of the fiber z, the axial variation of the modal birefringence can be expressed as the following Taylor series near the center of AO interaction length L,

$$\Delta n = \Delta n_0 + \sum_{l=1} \frac{\partial^{(l)}}{\partial z^{(l)}} \Delta n \cdot \frac{(z - L/2)^l}{l!}, \tag{7}$$

where, Δn_0 represent the modal birefringence at the center wavelength of λ_0 when the birefringence non-uniformity does not exist. In case that the torsional acoustic wave is applied to the device with constant wavelength, if Δn is not uniform but partly increase along the fiber axis as compared with Δn_0, the resonant phase matching condition is satisfied for $\lambda > \lambda_0$ and the polarization coupling is enhanced on the long wavelength side of the transmission spectra

#91710 - $15.00 USD Received 14 Jan 2008; revised 15 Mar 2008; accepted 15 Mar 2008; published 19 Mar 2008

of the filter. Otherwise, if Δn partly decreases along the fiber axis as compared with Δn_0, the resonant phase matching condition is satisfied for $\lambda < \lambda_0$ and the polarization coupling is enhanced on the short wavelength side of the transmission spectra of the device. However, it should be noted that the asymmetry in the sidelobe levels varies with not only the magnitude of the birefringence deviation but also its axial distribution in the AO interaction length of the filter [21, 22]. For instance, the Δn profile which has even components with respect to distance from the center of the AO interaction length exhibits sidelobe asymmetry. However, linear chirps or odd components in the Δn profile yield a symmetric broadening of the transmission peak with increased sidelobe levels because the polarization coupling is symmetrically enhanced in both wavelength regions on the center wavelength of λ_0. The sizable asymmetry observed in Fig. 5 suggests the existence of strong even component in the non-uniformity of birefringence. We calculated the amplitude of a quadratic Δn profile as the simplest example. The results shows the deviation is estimated to be 3.0×10^{-6} for the measured transmission spectra, which corresponds to the effects of a few-nm deviation in large hole diameter or in the distance between two large holes. Figure 5(b) shows the measured and calculated transmission spectra for the quadratic Δn profile.

Figure 6 shows the center wavelength change of the AOTPF as a function of the acoustic wavelength showing an almost linear relationship over the whole tuning range of 1530 - 1620 nm limited by the light source. The applied acoustic wavelength considered the dispersion properties of the lowest order torsional acoustic mode in the HB PCF agrees well with the polarization beatlength measured from the resonant phase matching condition in the transmission spectra.

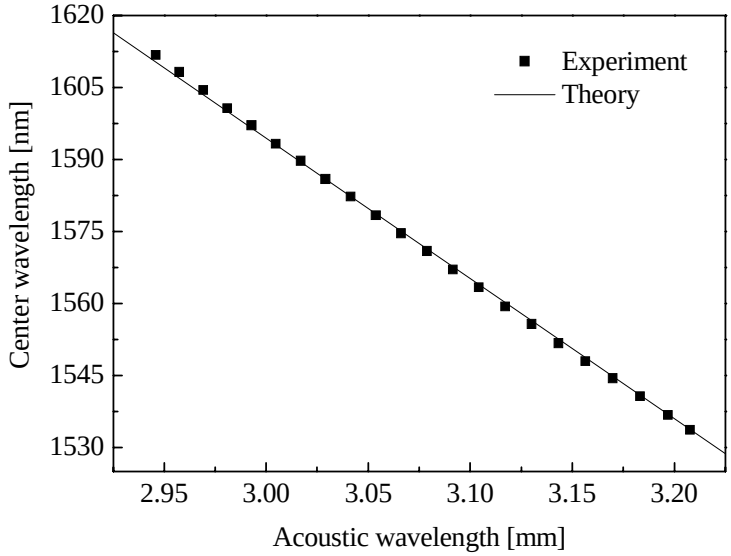

Fig. 6. Center wavelength of the all-fiber AOTPF as a function of the acoustic wavelength.

4. Conclusion

In conclusion, we have investigated the AO coupling properties between two optical polarization modes of the LP_{01} mode propagating in a HB PCF. A full coupling between two polarization modes was achieved over the wavelength range from 1530 nm to 1620 nm in an all-fiber AOTPF using the lowest order torsional acoustic mode. The coupling resonances are actively tunable both in the resonant wavelength and in the coupling strength by adjusting the acoustic frequency and the magnitude of the applying electric signal, respectively. We discussed the dispersion properties of the lowest order torsional acoustic mode in the PCF and

#91710 - $15.00 USD Received 14 Jan 2008; revised 15 Mar 2008; accepted 15 Mar 2008; published 19 Mar 2008

explained the source of the observed asymmetry in the sidelobe spectra in terms of the even-order variation of modal birefringence as a function of the distance from the center of AO interaction length of the filter.

Acknowledgments

The authors thank Prof. Wei Jin from the Department of Electrical Engineering in the Hong Kong Polytechnic University for providing the HB photonic crystal fiber used in this work.

#91710 - $15.00 USD Received 14 Jan 2008; revised 15 Mar 2008; accepted 15 Mar 2008; published 19 Mar 2008